Journal of Science and Transport Technology
Journal homepage: https://jstt.vn/index.php/en

The effect of tuned liquid damper placement on the seismic response of a high-rise building: A reduced-order modelling study

Thuong Anh Nguyen[1], An Le Hoang[2], Sang Pham Ngoc[2], Hoa Thi Trinh[3,*]
[1]Civil Engineer, EDF UK; thuong-anh.nguyen@edf.fr
[2]SDCT Research Group, Ho Chi Minh City University of Transport, Ho Chi Minh City, Vietnam; hoangan.le@ut.edu.vn, phamngocsang@ut.edu.vn
[3]Advanced Materials and Intelligent Systems for Infrastructure and High-Speed Rail (AMIS-HSR) research group, University of Transport Technology, Hanoi Vietnam; hoatt85@utt.edu.vn

Article info
Type of article:
Original research paper

DOI:
https://doi.org/10.58845/jstt.utt.2026.en.6.5.276-303

***Corresponding author:**
Email address:
hoatt85@utt.edu.vn

Received: 28/07/2026
Received in Revised Form: 17/10/2026
Accepted: 04/11/2026

Abstract: High-fidelity fluid–structure interaction (FSI) analysis is widely recognized as one of the most accurate approaches for evaluating the seismic performance of tuned liquid dampers (TLDs). However, coupling a three-dimensional FSI model with a detailed finite-element model of a high-rise building requires substantial computational resources, limiting its application in routine engineering analysis and preliminary design. This study develops and validates a computationally efficient reduced-order structural–FSI framework that preserves the dominant structural dynamic characteristics while explicitly modeling three-dimensional liquid sloshing. A 30-story reinforced-concrete building is first modeled in ETABS to extract its modal properties. The detailed structural model is subsequently transformed into an equivalent lumped mass–spring–damper system implemented in ANSYS and coupled with three-dimensional TLD fluid domains using FLUID80 elements. The reduced-order structural model reproduces the fundamental natural frequency of the full three-dimensional model with an error of less than 0.2%, demonstrating excellent agreement in the dominant dynamic response. Nonlinear time-history analyses are performed under the 1940 El Centro north–south earthquake record to investigate two practical TLD layouts: six tanks installed at the roof and a distributed configuration with three tanks at the roof and three at mid-height. Both configurations reduce global structural displacement and generally mitigate interstory drift and story shear, although local increases in drift or shear can occur at some floors. The roof-mounted configuration decreases the peak roof displacement from 0.389 m to 0.352 m (approximately 9.5%) and reduces the maximum base shear from 5.52 x 10^7 N to 5.22 x 10^7 N. Although the distributed configuration provides smaller global reductions, it offers improved response mitigation at intermediate stories through enhanced interaction with higher vibration modes. The proposed framework provides a mechanically consistent and computationally practical methodology for system-level seismic assessment and preliminary design of high-rise buildings incorporating tuned liquid dampers.

Keywords: Tuned liquid damper (TLD), reduced-order modeling, fluid–structure interaction, high-rise building, seismic assessment, nonlinear time-history analysis.

1. Introduction

The rapid development of high-rise buildings in densely populated urban areas has significantly increased the demand for reliable and efficient seismic vibration-control technologies. Owing to their slender structural configuration and relatively low lateral stiffness, reinforced concrete (RC) high-rise buildings generally possess long fundamental vibration periods, typically ranging from 0.2 to 0.4 Hz for structures with 20–40 stories [1], [2]. This frequency range often overlaps with the dominant frequency content of strong earthquake ground motions, making such structures particularly vulnerable to resonance-induced amplification. Consequently, excessive roof displacement, large interstory drift, and increased inertial forces may develop during seismic events, adversely affecting both structural integrity and the serviceability of nonstructural components.

To improve seismic resilience, various passive, semi-active, active, and hybrid vibration-control systems have been developed and implemented in modern structures, including tuned mass dampers (TMDs), viscous and friction dampers, and base-isolation systems [3]. Among these alternatives, tuned liquid dampers (TLDs) have attracted considerable attention because of their simple construction, low installation and maintenance costs, architectural compatibility, and ability to utilize existing water-storage tanks commonly located on rooftops or mechanical floors of high-rise buildings [4], [5]. Unlike conventional mechanical dampers, TLDs dissipate structural vibration energy through liquid sloshing inside partially filled tanks. Under seismic excitation, the interaction between the oscillating liquid free surface and the supporting structure converts structural kinetic energy into viscous dissipation, turbulence, wave breaking, and nonlinear free-surface deformation, thereby reducing structural responses.

Over the past three decades, extensive research has substantially advanced the understanding and practical application of TLD systems. Early investigations primarily focused on establishing the fundamental sloshing mechanism and validating the vibration-control capability of rectangular liquid tanks through analytical formulations and laboratory experiments [4-6]. These pioneering studies demonstrated that properly tuned liquid dampers could effectively reduce structural vibration under dynamic excitation, providing the theoretical basis for subsequent TLD design methodologies. Subsequent research investigated multiple-tank configurations with distributed sloshing frequencies to improve control robustness [7]. These studies were later extended to multi-degree-of-freedom structures and high-rise buildings [8], while numerical optimization methods were developed to determine the optimal tuning parameters, damper configurations, and mass ratios of single and multiple liquid-column dampers [9], [10]. These studies significantly improved TLD design strategies for practical engineering applications, particularly for wind-induced vibration control.

With the rapid development of computational mechanics and fluid dynamics, numerical simulation has become an indispensable tool for investigating TLD behavior under increasingly complex loading conditions. Recent studies have employed finite-element methods, computational fluid dynamics (CFD), and fluid–structure interaction (FSI) techniques to simulate nonlinear sloshing phenomena, including wave breaking, vortex formation, turbulent flow, and hydrodynamic pressure distributions that cannot be adequately represented by conventional analytical models [11-15]. These high-fidelity numerical approaches have substantially improved the physical realism of TLD simulations and provided valuable insights into the nonlinear interaction between liquid motion and structural vibration under strong dynamic excitation, including seismic loading.

Despite these significant advances, existing

research has also expanded toward practical implementation issues. Experimental investigations have demonstrated the effectiveness of TLD and tuned liquid column damper (TLCD) systems in reducing seismic responses of building structures [16], while numerical studies have explored innovative configurations, including elastically supported TLD systems and simplified finite-element models for seismic analysis [17], [18]. Furthermore, recent review studies have systematically summarized analytical, experimental, and numerical developments in TLD technology, highlighting the importance of liquid properties, tank geometry, and frequency tuning in achieving effective vibration mitigation [19]. Complementary numerical investigations have also examined detailed sloshing behavior in rigid liquid tanks subjected to dynamic loading using finite-element-based FSI formulations [20]. Collectively, these studies demonstrate the continuous evolution of TLD research from simplified analytical representations toward increasingly realistic numerical simulations and engineering-oriented applications.

A comprehensive summary of representative research conducted between 1990 and 2025 is presented in Table 1. The table illustrates the evolution of TLD research from early analytical formulations and small-scale experimental investigations to advanced CFD- and FSI-based numerical simulations, optimization techniques, and practical seismic applications. It also reveals the increasing emphasis on accurately representing nonlinear sloshing behavior and improving the effectiveness of liquid-based vibration-control systems for high-rise buildings while highlighting several remaining challenges that continue to motivate further investigation.

The literature summarized in Table 1 demonstrates that research on tuned liquid dampers has progressed substantially over the past three decades, evolving from simplified analytical formulations and laboratory-scale experiments to advanced finite-element, CFD, and fluid–structure interaction (FSI) simulations. These advances have significantly improved the understanding of sloshing dynamics and the vibration-control mechanisms of TLD systems under wind and earthquake excitations [4-6], [13-15]. Moreover, previous studies have investigated optimization strategies, hybrid TLD configurations, and practical implementation in high-rise buildings, providing valuable guidance for engineering design [7–10], [16 - 18].

Despite these developments, several important challenges remain unresolved.

First, many previous studies employed simplified analytical sloshing models, such as equivalent lumped-mass representations or linear wave theory, which cannot fully reproduce nonlinear free-surface deformation, wave breaking, turbulence, and the complex interaction between the liquid and its supporting structure under strong excitation [6], [11], [12], [21]. Although recent numerical and FSI-based models provide substantially improved representations of the coupled response of TLD–structure systems [13-15], they generally require greater modelling effort and computational resources than conventional equivalent mechanical models. These requirements can limit their applicability in routine engineering practice, extensive parametric studies, and preliminary structural design.

Second, the majority of previous investigations have considered rooftop installation as the default location for TLD systems [4], [5], [7], [14]. However, contemporary high-rise buildings frequently contain intermediate mechanical floors or service levels that can accommodate considerable water-storage capacity. The influence of TLD elevation on modal participation, the dynamic interaction between structural modes and liquid sloshing, and the overall vibration-control efficiency remain insufficiently quantified [17], [18], despite their practical significance for modern building design.

Third, previous studies have often focused on a limited number of structural response quantities, such as roof displacement, acceleration, or base shear [9], [16], [14]. A comprehensive assessment simultaneously considering global displacement, interstory drift, and story shear—which are key engineering demand parameters in performance-based earthquake engineering—remains relatively limited. Consequently, the overall effectiveness of different TLD layouts has not been fully understood from a system-level structural perspective.

To address these limitations, this study develops a computationally efficient hybrid structural–fluid modeling framework for seismic assessment of high-rise buildings equipped with tuned liquid dampers. Unlike conventional high-fidelity FSI models, the proposed methodology combines a reduced-order structural model, calibrated from a detailed three-dimensional ETABS model, with an explicit three-dimensional fluid domain implemented in ANSYS using a fully coupled FSI formulation. This hybrid strategy preserves the dominant structural dynamic characteristics while explicitly capturing nonlinear sloshing behavior, thereby achieving a practical balance between computational efficiency and physical fidelity.

A 30-story reinforced-concrete building is selected as the benchmark structure. Two representative TLD layouts are investigated under nonlinear time-history analysis using the 1940 El Centro earthquake record: (i) six tanks installed at the roof level and (ii) a vertically distributed configuration consisting of three tanks at the roof and three tanks at an intermediate floor. Rather than focusing on probabilistic seismic demand assessment, the study aims to evaluate the equivalence of the reduced-order structural representation, examine the influence of TLD placement on structural response, and assess the applicability of the proposed framework for system-level seismic analysis.

The principal scientific contributions of this study are summarized as follows: (1) A computationally efficient hybrid structural–FSI framework is developed by coupling a reduced-order structural representation with a fully three-dimensional fluid model, providing an effective compromise between computational cost and physical accuracy; (2) The reliability of the reduced-order structural model is verified through comparison with a detailed three-dimensional building model, demonstrating that the proposed equivalent representation preserves the dominant dynamic characteristics required for seismic response analysis; (3) The influence of TLD vertical placement on modal interaction and structural response is systematically investigated by comparing rooftop and vertically distributed layouts under identical seismic excitation; (4) A comprehensive system-level seismic evaluation is performed using multiple engineering demand parameters, including roof displacement, interstory drift, and story shear, providing practical guidance for performance-oriented analysis and preliminary design of high-rise buildings incorporating tuned liquid dampers. Overall, the proposed methodology bridges the gap between computationally intensive high-fidelity FSI simulations and simplified structural models commonly adopted in engineering practice. By combining computational efficiency with physically consistent fluid–structure interaction, the proposed framework provides a practical and reliable numerical tool for evaluating TLD performance in high-rise buildings under seismic loading.

2. Numerical Methodology

2.1. Computational framework

This study proposes a hybrid structural–fluid–structure interaction (FSI) computational framework for evaluating the seismic performance of high-rise buildings equipped with tuned liquid dampers (TLDs). As illustrated in Fig. 1, the proposed framework combines a reduced-order structural model (ROSM), developed from a

detailed three-dimensional finite-element (FE) model through dynamic equivalence, with a fully coupled three-dimensional fluid model established in ANSYS. The computational procedure consists of five sequential stages. First, a detailed FE model of the building is developed to determine its dynamic characteristics through modal analysis. Second, the extracted modal properties are employed to establish a reduced-order structural model that preserves the dominant dynamic behavior of the original structure while substantially reducing the computational cost. Third, the TLD is modeled using a three-dimensional fluid domain, with its sloshing frequency tuned to the fundamental natural frequency of the structure. Fourth, the structural and fluid models are integrated through a bidirectional FSI formulation to capture the interaction between structural vibration and liquid sloshing. Finally, nonlinear time-history analysis is performed to evaluate the seismic performance of different TLD configurations under earthquake excitation.

Table 1. Summary of major research on TLDs from 1990 to 2025

No.	Author(s)	Method	Structure / Model	TLDs Configuration	Key Findings/ Limitations	Limitations	Excitation
1	Fujino, Sun, Pacheco & Chaiseri (1992) [4]	Experimental + Analytical	Scaled building model	Rectangular sloshing TLD	Validated sloshing damping mechanism; 10%–25% displacement reduction; foundational TLD formulation	Small-scale model; limited to wind-type excitations	Mainly Wind
2	Reed et al. (1998) [6]	Experimental (shake table)	Multi-story steel frame	Rectangular water tanks	Strong nonlinear sloshing; wave breaking; damping depends on water depth	Did not model FSI explicitly	Seismic
3	Tait et al. (2005-2008) [5]	Experimental + Numerical	Multi-story building model	Tuned Liquid Dampers + arrays	Developed modern TLD design theory; 20%–22% displacement reduction	Simplified 2D sloshing assumptions	Wind + Seismic
4	Fujino and Sun (1993) [7]	Analytical and numerical	Structure–MTLD system	Multiple tuned liquid dampers with distributed sloshing frequencies	Demonstrated the effectiveness and robustness of MTLD systems; investigated frequency distribution and tuning characteristics	Based mainly on analytical/numerical modeling; detailed nonlinear wave breaking and explicit FSI were not considered	Harmonic /random excitation
5	Min et al. (2005) [8]	Numerical performance evaluation	76-story MDOF benchmark building	TLCD system	Significant reductions in wind-induced displacement and acceleration; performance depended on tuning, mass ratio, and head-loss coefficient	No detailed nonlinear sloshing, explicit FSI, or experimental validation	Wind
6	Mohebbi et al. (2015) [9]	Numerical + GA optimization	Ten-story MDOF shear frame	Multiple TLCDs	GA-optimized MTLCDs reduced peak displacement and acceleration; increasing damper number did not necessarily improve control	Simplified TLCD model; no free-surface wave breaking or explicit FSI	White noise and seismic

Table 1. (continued)

No.	Author(s)	Method	Structure / Model	TLDs Configuration	Key Findings/ Limitations	Limitations	Excitation
7	Gao et al. (1997) [10]	Numerical + parametric optimization	Simplified flexible structure	U-shaped TLCD	Determined optimum tuning and geometric parameters; response reduction depended strongly on frequency ratio and head loss	Harmonic loading only; no CFD or experimental validation	Harmonic
8	Chu et al. (2018) [13]	Experimental + 3D CFD/LES	Rigid rectangular water tank	Water tank with multiple vertical baffles	Experiments and large-eddy simulations quantified sloshing-induced hydrodynamic forces; baffles generated vortices and enhanced energy dissipation	Isolated rigid tank; no structural coupling; not a full-scale building TLD	Harmonic horizontal excitation
9	Shah & Usman (2022) [16]	Experimental shake-table testing	Small-scale four-storey steel MDOF frame	Roof-mounted U-shaped TLCD	TLCD significantly reduced RMS and peak floor accelerations, particularly near resonance, and remained effective under El Centro excitation	Small-scale steel model; single TLCD configuration; limited full-scale validation	Harmonic and seismic excitation
10	H.T, Trinh, T.T.T., Nguyen, 2020. [19]	Analytical + Review	General building structures	Classical rectangular sloshing TLD	Reviewed analytical, experimental, and numerical TLD design methods, emphasizing the key roles of liquid frequency, water depth, and tank geometry in vibration control of slender high-rise buildings.	Primarily a theoretical synthesis; no detailed FEM implementation for specific structural cases	Various dynamic loadings
11	H.T. Trinh, T.T.T. Nguyen, Nguyen, T.C., Nguyen, T.A., 2020. [20]	Numerical (FEM)	Rigid tank–liquid system	Rectangular water tank TLD	Used ANSYS FEM to simulate fluid–structure interaction and sloshing-induced hydrodynamic pressures under harmonic loading.	Tank–building interaction not considered; excitation limited to harmonic loading	Harmonic loading
12	H.T. Trinh, T.T.T., Nguyen, 2022. [17]	Numerical + Parametric	High-rise building with TLD	TLD with elastic (bonded cushion) support	Identified an optimal TLD–structure connection stiffness for maximizing seismic reductions in roof displacement and base shear.	Idealized elastic connection; material nonlinearity and damage not considered	Seismic
13	H.T.Trinh, & T.T.T., Nguyen, (2022) [18]	Numerical (Simplified FE Model)	High-rise building; simplified FE with FSI; El Centro (1940)	Rectangular TLD; varied geometry & water depth; optimized via frequency ratio	Best performance when frequency ratio ≈ 1; geometry and water depth strongly influence effectiveness	Single earthquake record; simplified model; no study on tank location or connection	Seismic

Table 1. (continued)

No.	Author(s)	Method	Structure / Model	TLDs Configuration	Key Findings/ Limitations	Limitations	Excitation
14	Tuong et al. (2019) [14]	Numerical analysis with FSI consideration	Multistory structure	Structure-mounted TLD	Evaluated structural responses and effects of TLD parameters	Simplified fluid representation; not high-resolution 3D CFD	Dynamic/ seismic
15	Eswaran et al. (2017) [15]	Partitioned FSI simulation + experiment	Three-storey model	TLD arrangement	Numerical predictions agreed with experiments; confirmed importance of proper tuning	Reduced-scale model; limited representation of turbulence and wave breaking	Harmonic and random

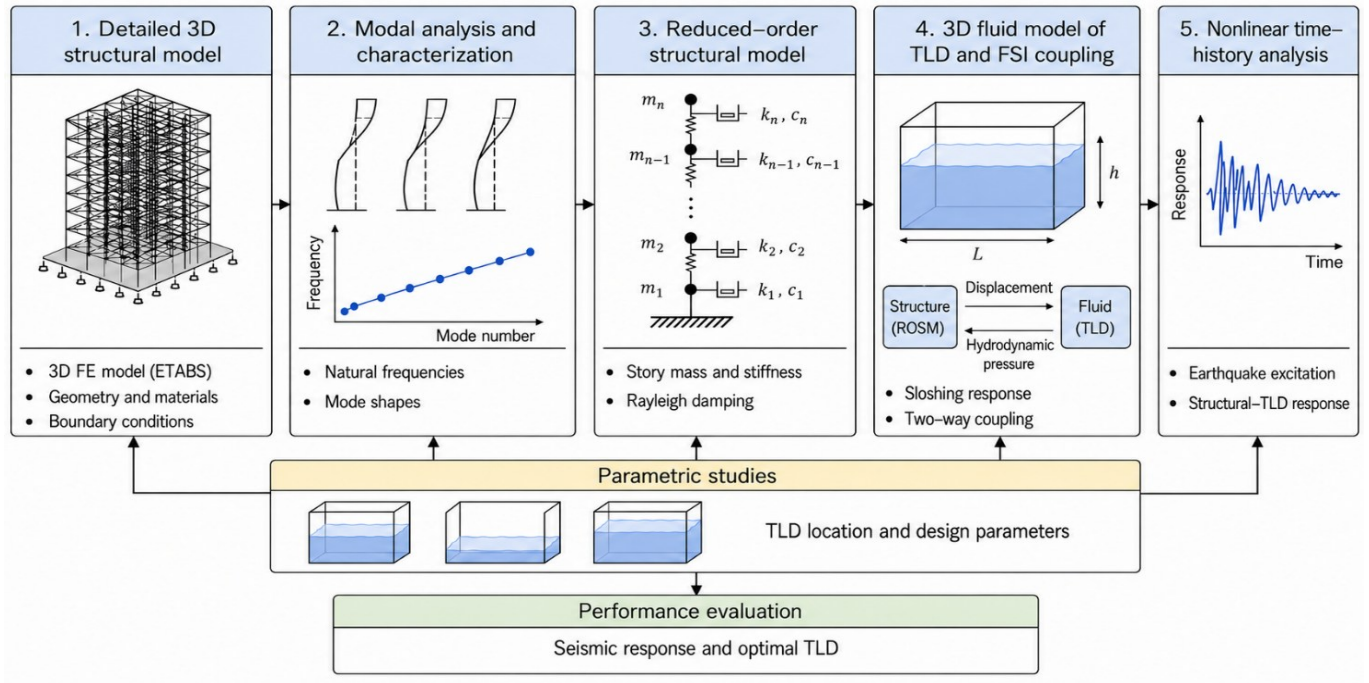


Fig. 1. Proposed simulation workflow

The proposed computational framework combines the efficiency of the reduced-order structural model with the accuracy of three-dimensional FSI analysis, providing an effective and computationally efficient approach for evaluating the seismic response of high-rise buildings equipped with TLDs.

2.2. Structural modeling and modal analysis

A detailed three-dimensional finite-element (FE) model of the building is first established to accurately represent the structural geometry, material properties, stiffness distribution, and mass distribution. Modal analysis is subsequently performed to determine the dynamic characteristics of the structure, which serve as the basis for both the development of the reduced-order structural model and the tuning of the TLD.

The modal analysis provides the following dynamic parameters:

f_i: natural frequency of the i-th vibration mode;

ϕ_i: mode shape of the i-th vibration mode;

Γ_i: modal participation factor of the i-th vibration mode.

These modal properties are subsequently employed to develop the equivalent reduced-order structural model described in the following section. In addition, the fundamental natural frequency of

the structure is adopted as the target frequency for tuning the TLD to maximize vibration mitigation under seismic excitation.

2.3. Development of the reduced-order structural model

To improve computational efficiency while preserving the dominant dynamic characteristics of the structure, the detailed FE model is transformed into an equivalent reduced-order structural model (ROSM) represented by a lumped mass–spring–damper (M–K–C) system. In this model, each story is idealized as a lumped mass connected by equivalent lateral springs and damping elements, thereby significantly reducing the number of degrees of freedom while maintaining the global dynamic response of the original structure. The equivalent lateral stiffness of each story is determined from the interstory stiffness relationship:

$$K_i = \frac{F}{H_{i+1} + \frac{V_{i+1} h}{B}} \quad (1)$$

where F is the applied lateral force at story i + 1; H_{i+1} is the lateral displacement at story i+1; V_{i+1} is the corresponding vertical displacement; h is the story height; and B is the floor width along the loading direction. This formulation considers both the shear deformation (H_{i+1}) and the flexural deformation ((V_{i+1}) h/B) of the structural system.

Here, computational efficiency refers to the reduction in structural degrees of freedom and equation-system size; a direct runtime comparison with the complete three-dimensional structural–FSI model was not performed under identical hardware and solver settings.

Rayleigh Damping Model

The damping matrix of the reduced-order structural model is represented using the Rayleigh proportional damping model to account for equivalent viscous damping in the dynamic analysis. The damping matrix is expressed as a linear combination of the mass and stiffness matrices [22]:

$$[C] = \alpha[M] + \beta[K] \quad (2)$$

where [M] and [K] denote the mass and stiffness matrices, respectively, while α and β are the Rayleigh damping coefficients. Proportional damping models have also been employed in finite-element analyses of liquid-containing structures subjected to horizontal and vertical ground motions [23], [24].

Transforming the system to modal coordinates using the modal matrix Φ yields:

$$[\Phi]^T [C][\Phi] = \alpha[1] + \beta[\omega^2] \quad (3)$$

Rayleigh damping can be employed in both linear and nonlinear dynamic analyses, although the damping coefficients and stiffness formulation must be selected carefully in nonlinear applications.

Modal damping ratio

The damping ratio of the i-th vibration mode is expressed as:

$$\xi_i = \frac{\alpha}{2\omega_i} + \frac{\beta\omega_i}{2} \quad (4)$$

where ξ_i: damping ratio of mode i; $\omega_i = 2\pi f_i$: circular natural frequency.

Determination of Rayleigh coefficients

If the damping ratios for two vibration modes i and j are known (ξ_i and ξ_j), the Rayleigh coefficients α and β can be computed using the matrix relation:

$$\begin{Bmatrix} \alpha \\ \beta \end{Bmatrix} = \frac{2\omega_i\omega_j}{\omega_j^2 - \omega_i^2} \begin{pmatrix} \omega_j & -\omega_i \\ -\frac{1}{\omega_j} & \frac{1}{\omega_i} \end{pmatrix} \begin{Bmatrix} \xi_i \\ \xi_j \end{Bmatrix} \quad (5)$$

For the common case where the same damping ratio $\xi_i = \xi_j = \zeta$ is assigned to both modes, Eq. (5) reduces to:

$$\alpha = \zeta \frac{2\omega_i\omega_j}{\omega_i + \omega_j}, \beta = \zeta \frac{2}{\omega_i + \omega_j} \quad (6)$$

The resulting Rayleigh damping curve ξ(ω) illustrates the characteristic shape: a rapid decay at low frequencies followed by a near-linear increase at higher frequencies, as shown in Fig. 2.

2.4. TLD modeling

The tuned liquid damper (TLD) is modeled as a partially filled rectangular tank in which vibration

energy is dissipated through liquid sloshing. The tank dimensions are selected such that the fundamental sloshing frequency approaches the fundamental natural frequency of the structure, thereby maximizing the vibration mitigation effect through resonance. Based on the linear wave theory, the fundamental sloshing frequency is calculated as

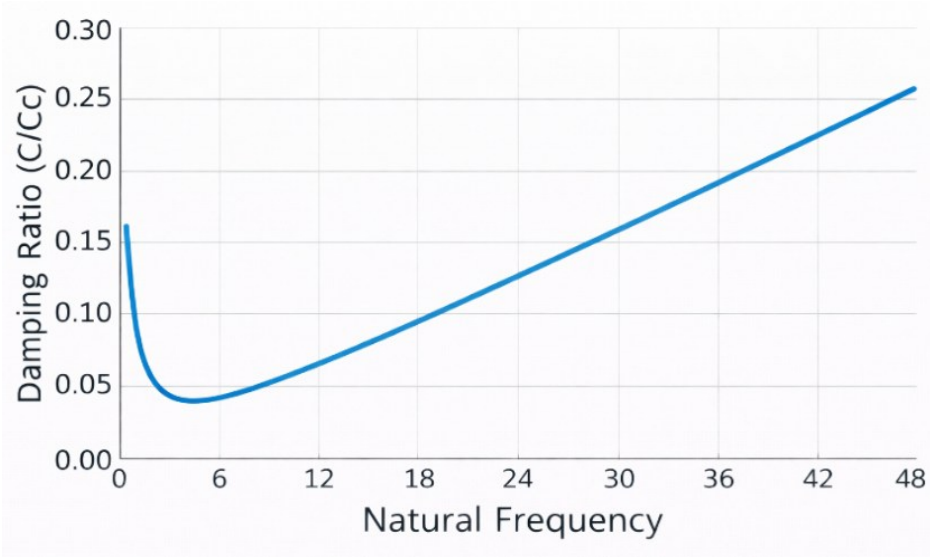


Fig. 2. Relationship between damping ratio and natural frequency of the structure [22]

$$f_s=\frac{1}{2\pi}\sqrt{gk_1\tanh(k_1h)} \qquad k_1=\frac{\pi}{L} \qquad (7)$$

where L is the tank length, h is the water depth, g is the gravitational acceleration, and k_1 is the first-mode wave number. The calculated sloshing frequency serves as the primary design parameter for tuning the TLD.

2.5. Fluid–structure interaction analysis

The interaction between the structural system and the TLD is simulated using a fully coupled fluid–structure interaction (FSI) formulation. The liquid domain is discretized using FLUID80 elements implemented in ANSYS APDL [25], while the free surface is represented using surface-effect elements capable of capturing nonlinear sloshing behavior and the corresponding hydrodynamic pressure.

The structural nodes at the tank base are kinematically coupled with the adjacent fluid elements, allowing the bidirectional transfer of displacement and hydrodynamic pressure during seismic excitation. This coupling strategy enables realistic simulation of the interaction between structural vibration and liquid sloshing throughout the dynamic response.

2.6. Nonlinear seismic response analysis

Finally, nonlinear time-history analysis is performed using the coupled structural–TLD model to evaluate the seismic performance of the proposed system. Earthquake excitation is applied at the base of the reduced-order structural model, and the dynamic response is solved using the Newmark–β time integration algorithm.

The effectiveness of the TLD configurations is evaluated using several engineering demand parameters, including roof displacement, interstory drift, story shear, and free-surface sloshing amplitude. The proposed computational framework therefore enables a systematic comparison of different TLD arrangements while maintaining both computational efficiency and simulation accuracy.

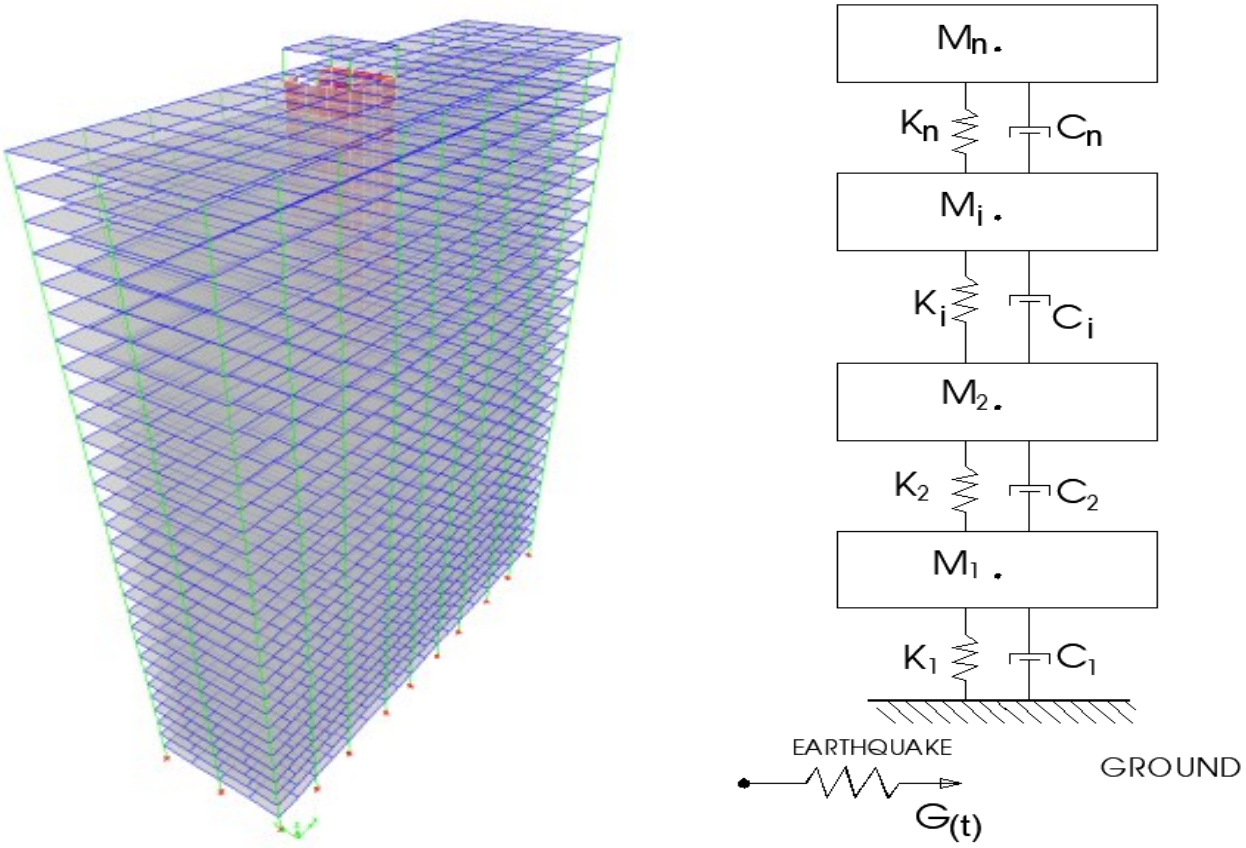
3. Structural and TLD System Modeling

This section presents the numerical models and input parameters employed in the nonlinear time-history analyses, including the structural model, modal characteristics, equivalent lumped mass–spring–damper representation, earthquake excitation, and the configuration of the TLD. Whereas the methodology section established the theoretical framework, the present section

describes the complete set of modeling assumptions and parameters used in the simulation of the 30-story reinforced concrete building. These include the structural geometry, mass and stiffness distributions, dynamic properties, the reduced-order model adopted for the time-history analyses, and the detailed characteristics and placement of the TLD system. Together, these components form the integrated structural–fluid dynamic model used to assess the seismic mitigation performance of the TLD configurations considered in this study.

3.1. Building Model, Modal Properties, and Equivalent Dynamic Representation

The prototype structure is a 30-story reinforced concrete office building with a total height of 108 m and plan dimensions of 58.8 m x 22 m. The lateral load-resisting system consists of RC shear walls and moment-resisting frames. Material properties, gravity loads, and wall thicknesses are defined according to the architectural and structural design documentation.



(a) 3D model on ETABS

(b) Equivalent model of the building including springs and dampers

Fig. 3. Finite-element model of the 30-story RC building and Equivalent lumped mass–spring–damper representation of the building

A detailed FE model was constructed in ETABS using frame and shell elements to represent beams, slabs, columns, and shear walls. Rigid diaphragm constraints were assigned at each floor level. The global structural configuration is illustrated in Fig. 3a, a global ETABS finite element model.

Model analysis was performed using the mass source combination [26–30]:

COMBO = SW + SDL + WDL + 0.25LL

where SW, SDL, WDL, and LL denote self-weight, slab dead load, wall dead load, and live load, respectively.

The model analysis results show that the building exhibits three main modes of vibration: lateral translation in the Y direction at a frequency

of 0.276 Hz, longitudinal translation in the X direction at a frequency of 0.299 Hz, and torsional vibration at a frequency of 0.320 Hz. These frequencies are within the typical range of high-rise reinforced concrete buildings, and the combination of the translational and torsional modes reflects the inherent stiffness asymmetry. Representative mode shapes are shown in Table 2.

Table 2. Table of natural vibration parameters of the structure

Mode	Period	Frequency	UX	UY	Sum UX	Sum UY	RX	RY	RZ	Sum RX	Sum RY	Sum RZ
1	3.62	0.276	0.00	66.96	0.00	66.96	98.89	0.00	0.00	98.89	0.00	0.00
2	3.35	0.299	37.5	0.00	37.49	66.96	0.00	50.98	37.10	98.90	50.99	37.10
3	3.13	0.320	34.9	0.00	72.35	66.96	0.00	48.75	38.42	98.90	99.73	75.52
4	1.09	0.921	3.1	0.00	75.41	66.96	0.00	0.00	7.60	98.90	99.73	83.12
5	0.96	1.043	10.6	0.00	85.98	66.96	0.00	0.03	2.67	98.90	99.76	85.79
6	0.91	1.102	0.00	15.95	85.98	82.91	0.73	0.00	0.00	99.62	99.76	85.79
7	0.60	1.661	0.57	0.00	86.55	82.91	0.00	0.03	3.53	99.62	99.79	89.32
8	0.49	2.035	4.01	0.00	90.56	82.91	0.00	0.17	0.59	99.62	99.96	89.91
9	0.40	2.512	0.27	0.00	90.83	82.91	0.00	0.00	2.00	99.62	99.96	91.91
10	0.39	2.554	0.00	6.28	90.83	89.19	0.29	0.00	0.00	99.91	99.96	91.91
11	0.32	3.162	2.21	0.00	93.04	89.19	0.00	0.01	0.22	99.91	99.97	92.14
12	0.28	3.525	0.12	0.00	93.16	89.19	0.00	0.00	1.46	99.91	99.97	93.60

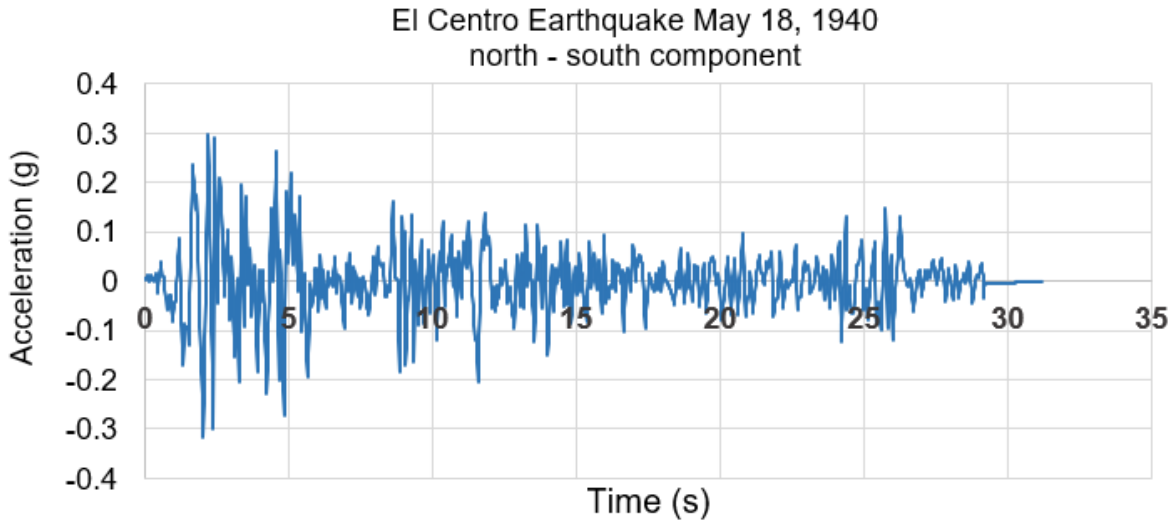


Fig. 4. Seismic input motion of a recorded signal during El Centro earthquake [31]

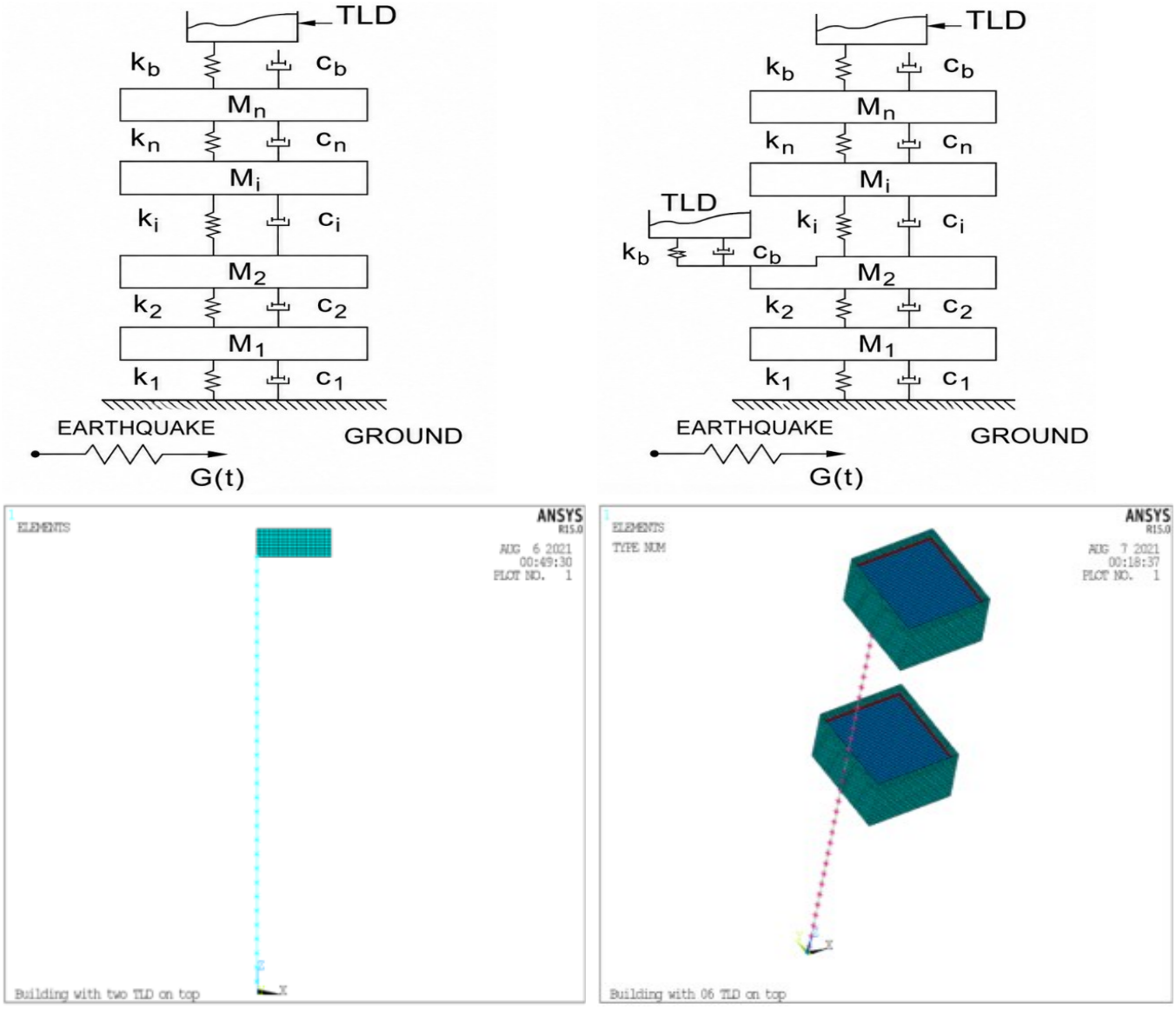
To perform nonlinear time-history analysis, the FE model was transformed into a lumped mass–spring–damper representation. In this equivalent model, the floor masses are concentrated at discrete nodes, interconnected by story stiffness and damping elements calibrated to reproduce the global dynamic characteristics of the ETABS model. The equivalent dynamic representation is illustrated in Fig. 3b, which shows the mass, stiffness, and damping configuration along the building height.

Interstory stiffness values were calibrated to reproduce the global lateral stiffness distribution obtained from the full ETABS model. Specifically, the first 15 stories (Stories 1–15) were assigned an interstory stiffness of 4.92 x 10^9 N/m, reflecting the higher stiffness of the lower structural region where the shear walls contribute most significantly to lateral resistance. In contrast, the upper 15 stories (Stories 16–30) were assigned a reduced stiffness

of 3.32 x 10^9 N/m, consistent with the natural tapering of wall thickness, reduced tributary mass, and the smaller shear demand in the upper portion of the building.

Rayleigh damping coefficients were selected to achieve a 5% damping ratio at the dominant modal frequencies. Validation of the equivalent model confirmed that its fundamental frequency (0.2765 Hz) closely matches that of the original FE model, ensuring that the reduced-order representation accurately preserves the dynamic characteristics of the full structural system.

3.2. Earthquake excitation and ground-motion characteristics



(a) Analytical model when 6 tanks are placed on the 30th floor

(b) Analytical model when 3 tanks are placed on the 30th floor, and 3 tanks are placed on the 15th floor

Fig. 5. ANSYS APDL models for analyzing the effects of water tanks

The system was subjected to the north–south component of the 1940 El Centro earthquake [31]. The acceleration–time history of this record, shown in Fig. 4, demonstrates the strong-motion nature of the event, with a peak ground acceleration of approximately 0.3g and an effective shaking duration of around 30 seconds.

The frequency content of the record contains substantial energy between 0.1 and 0.3 Hz, a range that overlaps significantly with the building's

fundamental vibration modes. This spectral compatibility makes El Centro an effective input for evaluating vibration mitigation performance, as it tends to excite both lateral and torsional components of tall buildings. The broad-band nature of the signal with rapid variations in acceleration, velocity, and displacement also provides a demanding test for assessing interstory drift response and the ability of supplemental damping devices to dissipate seismic energy.

3.3. TLD configuration and fluid–structure interaction modeling

The TLDs were designed such that the sloshing frequency of the water approaches the first natural frequency of the structure. Each tank has plan dimensions of 8.5 m x 8.5 m, a water depth of 3.2 m, a wall height of 4.0 m, and a total mass of 387.4 tons. With six tanks installed, the overall TLD-to-structure mass ratio equals 3.469%, which lies within the optimal range commonly reported in the literature.

Two configurations were investigated:

(1) installation of all six tanks at the roof level, and

(2) a split configuration, with three tanks at the roof and three at mid-height (15th floor).

These two TLD arrangements are illustrated in Fig. 5, enabling comparison of the effects of vertical mass distribution.

The liquid domain inside each tank was modeled using FLUID80 elements in ANSYS [25], capable of simulating free-surface deformation and hydrodynamic pressure fields. Full coupling between the tank base nodes and the structural nodes ensures that sloshing-induced forces are transferred accurately into the structural model. Interaction stiffness and damping coefficients were implemented to capture both impulsive and convective components of fluid motion, providing a realistic representation of TLD behavior under seismic loading.

4. Model validation

To ensure the reliability of the numerical framework, the simplified lumped mass–spring–damper model used in the ANSYS APDL time-history analysis was validated against the full 3D-FE model developed in ETABS. The validation focuses on the comparison of natural frequencies and modal participation characteristics, as these are the primary determinants of structural response and TLD tuning performance.

4.1. Validation of structural dynamic properties

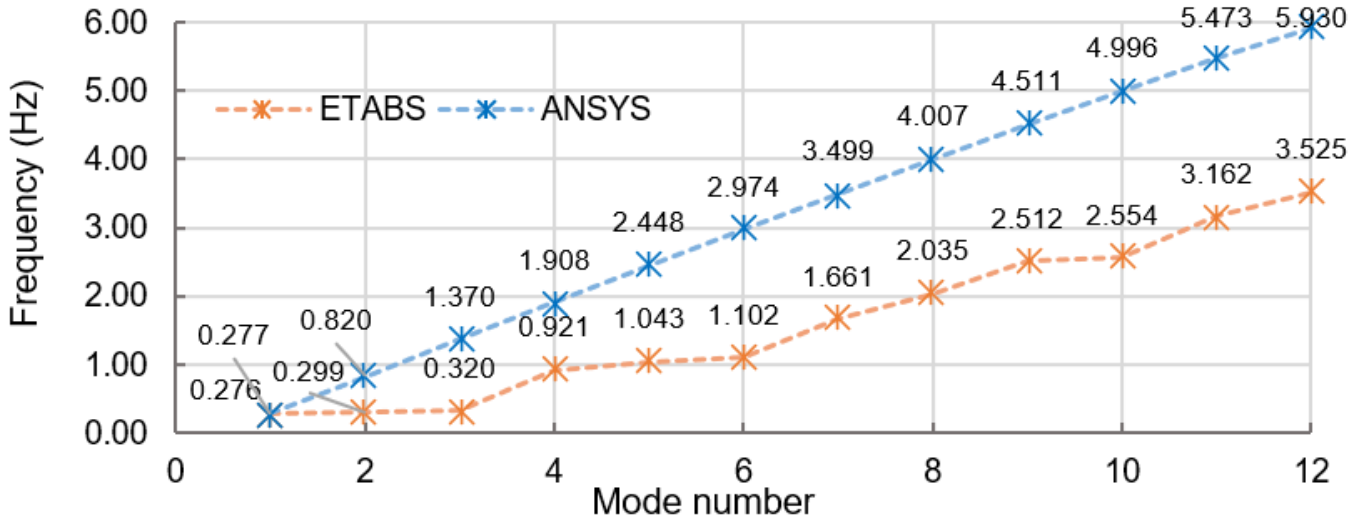


Fig. 6. Comparison of the First 12 Natural Frequencies: ETABS vs. ANSYS

A validation study was conducted to assess the fidelity of the equivalent lumped-mass model by comparing its dynamic characteristics with those obtained from the full 3D ETABS model. Fig. 6 presents a mode-by-mode comparison of the first twelve natural frequencies derived from both

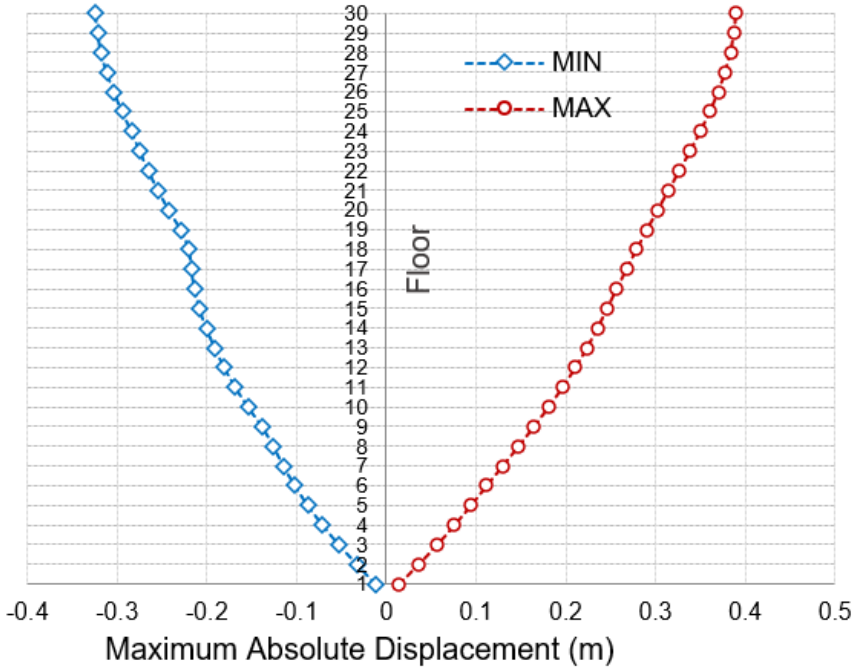
models. The fundamental frequency predicted by the equivalent model (0.277 Hz) shows excellent agreement with the ETABS result (0.276 Hz), corresponding to a discrepancy of less than 0.2%. This close match indicates that the equivalent model reproduces the dominant lateral dynamic characteristics of the detailed structure; however, agreement in natural frequency alone does not establish equivalence of torsional mode shapes. For the second and third modes (identified in the full ETABS model as X-direction translation and torsion, respectively), the corresponding frequency deviations are reported to be within 1%–3%, which is well within the acceptable bounds for simplified models commonly employed in seismic response analyses. As expected, higher-order modes exhibit larger discrepancies, typically between 10% and 20%, primarily due to simplifications inherent in the equivalent representation, such as rigid diaphragm assumptions, the omission of torsional–flexural coupling, and the reduction of distributed stiffness into discrete story springs. Nevertheless, these differences have minimal influence on the global seismic response because higher modes contribute significantly less to overall mass participation. A comparison of modal mass participation further confirms the consistency between the two modeling approaches. The first translational mode of the ETABS model mobilizes 66.96% of the effective mass, whereas the equivalent model captures more than 81% in the same direction. This difference arises because the ETABS model retains three-dimensional translational and rotational degrees of freedom, whereas the reduced-order model retains only the principal lateral translation at each floor. Consequently, a larger proportion of the retained directional mass participates in the first translational mode of the reduced-order model. Given that the seismic response of tall RC buildings is typically dominated by the fundamental mode, this level of agreement ensures that the equivalent model is sufficiently accurate for nonlinear time-history analyses and for evaluating the performance of TLD. Overall, the validation confirms that the simplified model retains the essential dynamic characteristics necessary for the subsequent parametric studies.

4.2. Discussion of modeling assumptions

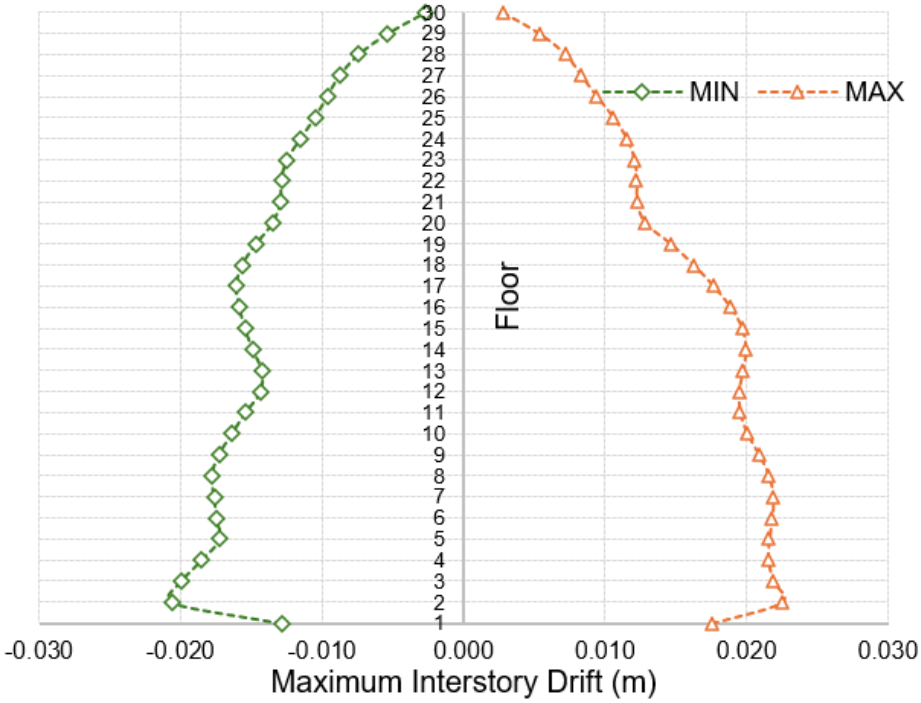
The construction of the equivalent lumped-mass model is founded on a set of mechanical idealizations designed to isolate the dominant lateral response mechanisms of the building. Vertical displacements and rotational degrees of freedom were excluded because, in a high-rise system governed primarily by shear and flexural deformation of walls and columns, these DOFs contribute negligibly to the global seismic response. The assumption of rigid floor diaphragms further reinforces this reduction, ensuring that lateral inertia forces are transmitted predominantly through story-level translations.

The representation of mass as lumped at story levels reflects the physical reality that inertial forces during earthquake excitation concentrate at floors, where the majority of the structural and nonstructural mass resides. This mass-lumping scheme is consistent with classical shear-building theory and preserves the relationship between story shear, interstory drift, and modal mass participation. Vertical stiffness was neglected on the basis that axial deformation in concrete walls and columns is orders of magnitude smaller than horizontal deformation; hence, its influence on the lateral stiffness matrix is minimal. Removing this component allows the equivalent model to remain computationally efficient without sacrificing fidelity in the modes that control TLD–structure interaction. Only the lateral DOF along the principal axis of vibration was retained, ensuring that the model captures the first translational mode, which governs more than two-thirds of the total mass participation in the ETABS model and over 80% in the equivalent model. Since the TLDs are tuned to this mode, preserving its frequency and modal shape is essential.

Comparison with the ETABS modal results demonstrates that these idealizations successfully retain the relevant physics of the structural system. The first-mode frequency is reproduced with near-perfect accuracy, and although higher-mode differences emerge due to the omission of torsional–flexural coupling and diaphragm deformability, they remain within acceptable limits for performance assessment. The equivalent model therefore provides a reliable and mechanically meaningful representation of the building's dynamic behavior, forming a robust basis for the subsequent nonlinear time-history analyses involving TLD.



(a) Maximum Absolute Displacement Profile of the Structure Without TLDs.



(b) Maximum Interstory Drift Between Adjacent Floors in the Uncontrolled Condition (without TLDs).

Fig. 7. Graph of Maximum Absolute Displacement and Maximum Relative Displacement between adjacent floors without water tank

5. Results and discussion

This section presents the seismic response of the 30-story reinforced concrete (RC) building subjected to the 1940 El Centro NS earthquake record, and evaluates the effectiveness of two TLD configurations: (i) six tanks installed at the roof level and (ii) a split configuration with three tanks at the roof and three at mid-height. The analyses focus on floor displacement, interstory drift, acceleration demand, and the global vibration mitigation achieved by the liquid damping system.

5.1. Structural response of the building without TLD

The seismic response of the 30-story reinforced concrete building subjected to the 1940 El Centro NS ground motion is dominated by the fundamental translational mode, which governs the global lateral deformation of the structure. As illustrated in Fig. 7a, the maximum absolute displacement increases almost monotonically from the base to the roof, reaching its peak value at the top floor. This displacement pattern is characteristic of a shear-type high-rise building, where the lateral deformation accumulates progressively along the height as a consequence of the increasing tributary mass and the continuous transfer of inertial forces through the structural system. The smooth displacement profile further indicates that the global dynamic response remains primarily controlled by the first vibration mode without significant modal irregularities. Although the overall displacement develops gradually over the building height, the deformation demand is not uniformly distributed. As shown in Fig. 7b, the maximum interstory drift is concentrated in the lower stories, particularly between the first and second floors, where the peak drift reaches approximately 22 mm. This behavior suggests that the lower structural levels experience the largest deformation gradient despite exhibiting relatively small absolute displacements. From a structural mechanics perspective, interstory drift represents the relative deformation between adjacent floors rather than the total lateral displacement; therefore, it is governed by the local balance between story stiffness and transmitted seismic shear. The concentration of drift near the base indicates that the seismic energy is primarily dissipated through deformation of the lower structural components, making these stories the most critical locations for potential stiffness degradation, cracking, and nonlinear damage initiation.

The distribution of story shear shown in Fig. 8 provides further insight into the internal force transfer mechanism during seismic excitation. The maximum shear demand occurs in the lower stories and decreases progressively toward the roof, following the typical response of shear-dominated high-rise buildings. This trend reflects the cumulative nature of inertial loading, whereby each lower floor must resist not only its own inertia force but also the combined inertial forces transmitted from all stories above. Consequently, the base region experiences the highest internal force demand and becomes the primary load-transfer zone during earthquake excitation. The slight asymmetry between the positive and negative shear envelopes originates from the non-symmetric characteristics of the El Centro ground motion rather than from any structural irregularity.

A clear mechanical correlation can be observed between the drift and shear distributions. The concentration of both quantities in the lower stories is consistent with the fundamental equilibrium relationship of shear-type structures, where the interstory deformation is directly associated with the balance between story shear and lateral stiffness. In other words, larger seismic shear acting on stories with finite stiffness inevitably results in greater relative deformation. This agreement confirms that both deformation-based and force-based response indices consistently identify the lower portion of the building as the most critical seismic region.

The uncontrolled structural response

demonstrates that seismic demand is concentrated in two distinct forms: global displacement accumulates toward the roof, whereas local deformation and internal force demands are concentrated near the base. This dual response mechanism highlights the necessity of introducing supplemental damping devices capable of simultaneously reducing global vibration amplitude and alleviating localized deformation demand in the critical lower stories.

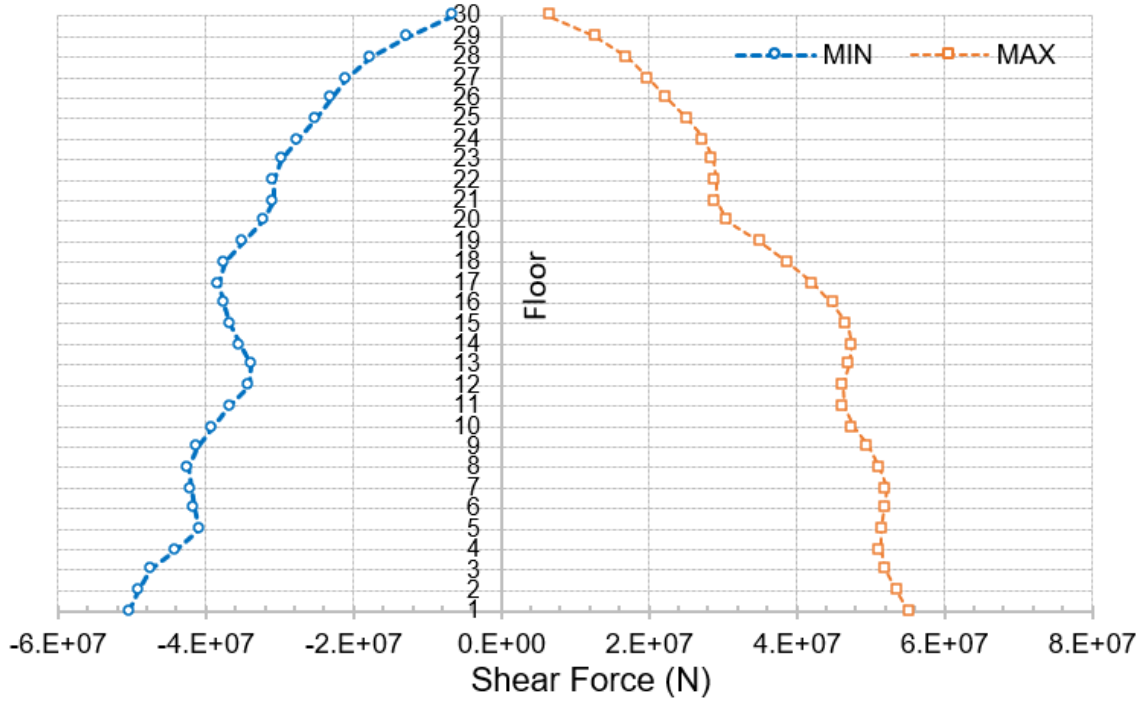
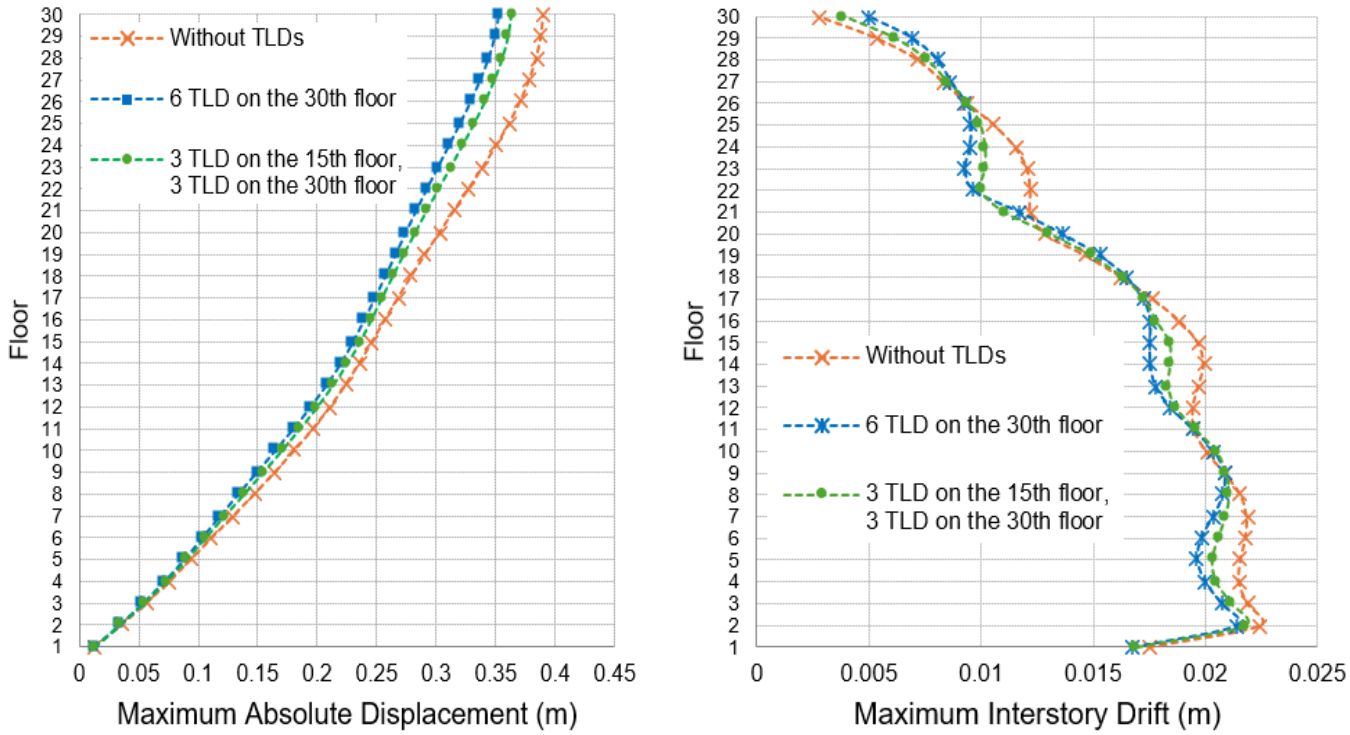


Fig. 8. Graph of maximum and minimum shear force values at floors without water tank



a) Maximum Absolute Displacement b) Maximum Interstory Drift Between Adjacent Floors

Fig. 9. Graph of maximum absolute displacement and maximum relative displacement between adjacent floors with water tank

5.2. Structural response of the building with tuned liquid tanks

The installation of tuned liquid dampers (TLDs) substantially modifies the dynamic characteristics of the building by introducing additional passive damping through the interaction between structural vibration and liquid sloshing. Two TLD arrangements were investigated: (i) six tanks installed on the roof (30th floor), and (ii) a distributed configuration consisting of three tanks on the 15th floor and three tanks on the roof. As illustrated in Fig. 9a, both configurations reduce the maximum absolute displacement throughout the building height compared with the uncontrolled structure, confirming the effectiveness of the TLD system in suppressing global lateral vibration.

The reduction in displacement is more pronounced when all six tanks are installed at the roof. This behavior is primarily associated with the dominant first translational mode, in which the largest modal displacement occurs at the top of the structure. Locating the TLDs at the point of maximum modal participation enhances the dynamic coupling between the oscillating liquid and the structural motion, allowing a greater portion of the input seismic energy to be transferred from the structure to the sloshing fluid and subsequently dissipated through viscous fluid motion. In contrast, although the distributed configuration also contributes to vibration reduction, relocating part of the liquid mass to the mid-height decreases its participation in the first-mode response, resulting in a slightly lower control efficiency.

The influence of the TLDs on local deformation is further demonstrated by the interstory drift profiles shown in Fig. 9b. Both TLD configurations reduce the drift demand over nearly the entire height of the building, with the most noticeable improvement occurring in the lower and middle stories where seismic deformation is most concentrated. This trend indicates that the TLDs not only reduce the overall structural displacement but also alleviate deformation gradients between adjacent floors. From a structural mechanics perspective, the reduction in interstory drift reflects a more uniform redistribution of lateral deformation along the building height, thereby decreasing the likelihood of localized stiffness degradation, cracking, and plastic hinge formation in critical lower-story structural members. Although the distributed arrangement provides comparable drift reduction over several middle stories, the roof-only configuration consistently exhibits slightly lower peak drift values because of its stronger interaction with the dominant vibration mode.

The effectiveness of the TLD system is also reflected in the story shear distributions presented in Fig. 10. Both TLD layouts generally reduce story shear demand, particularly over much of the lower building height; however, local increases in the shear envelope occur at some upper floors, especially for the six-TLD rooftop configuration (Fig. 13). Since story shear is directly governed by the dynamic inertia forces generated during structural vibration, the reduction in shear indicates that the TLDs effectively decrease the acceleration response of the building by dissipating part of the seismic input energy. Consequently, the lateral force demand may decrease at many story levels, although reductions in the internal forces of individual structural members cannot be assumed uniformly from these story-shear results. The rooftop configuration provides stronger global displacement control, but it does not produce the greatest story-shear reduction at every floor.

Overall, both TLD arrangements improve global displacement response and generally mitigate interstory drift and story shear, although local increases in drift or shear may occur at particular floors. The roof-only configuration is more effective in reducing global displacement through stronger interaction with the dominant first vibration mode, whereas its relative benefit for local drift and story shear varies with floor level. These results suggest that roof-level placement may be preferable when global displacement reduction is

the primary objective, but floor-specific drift and shear demands should also be checked when selecting a TLD layout.

5.3. Effect of TLD placement on seismic response modification

To quantify the influence of TLD placement on the seismic response at each floor, the relative response change ratio is defined as:

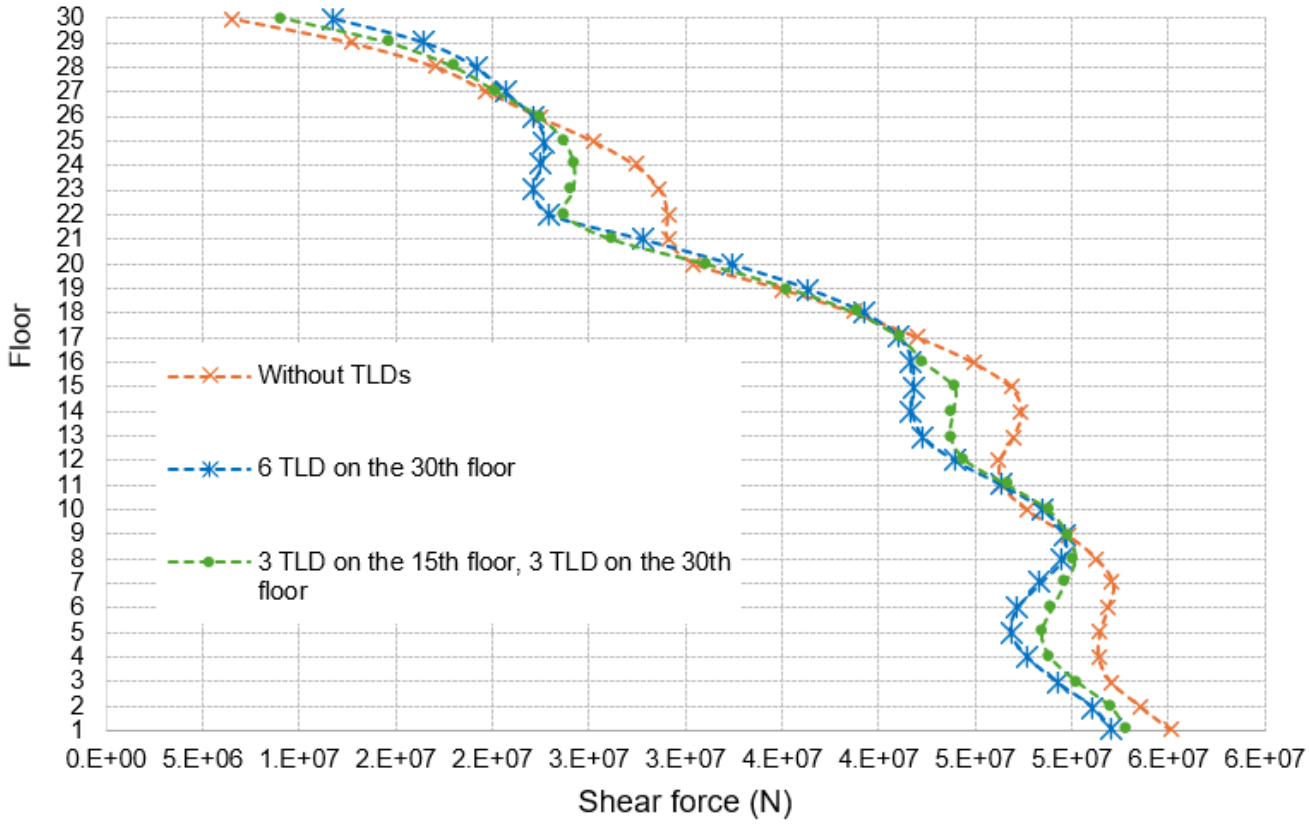


Fig. 10. Graph of maximum and minimum shear force values at floors with water tank

$$R_{(i)}=\frac{R_{(i)_TLD}-R_{(i)_noTLD}}{R_{(i)_noTLD}}\times 100(\%) \quad (8)$$

where $R_{i,\,noTLD}$ and $R_{i,\,TLD}$ denote the peak response at the i-th floor for the uncontrolled and TLD-controlled structures, respectively. The response envelope is evaluated from the larger absolute value of the positive and negative extrema:

$$R_i = \max\left(R_{i,max}, |R_{i,min}|\right)$$

Under this definition, a negative value indicates a reduction relative to the uncontrolled structure, whereas a positive value represents a local increase. This formulation allows the floor-by-floor effectiveness of the two TLD layouts to be evaluated independently of the magnitude of the original response.

5.3.1. Modification of absolute displacement

Fig. 11 shows that both TLD configurations reduce the peak absolute displacement over the entire building height. The reduction is not spatially uniform, however, indicating that control efficiency depends on the interaction between the TLD location and the structural modal deformation. The configuration with six TLDs at the roof provides the larger displacement reduction, particularly in the upper half of the building. The maximum reduction occurs approximately around Floors 24–26, where the roof-mounted system decreases the displacement by about 11–12%, compared with approximately 8% for the distributed arrangement. At the roof, the corresponding reductions are approximately 10% and 7%, respectively.

This response pattern can be explained by the first-mode deformation of the building. Since the modal displacement increases toward the roof, TLDs located at the top experience a larger support motion and therefore develop a stronger relative

liquid motion. The enhanced sloshing response increases the transfer of vibration energy from the structure to the liquid and produces a larger out-of-phase hydrodynamic restoring force. Consequently, concentrating the complete liquid mass at the roof maximizes the generalized damping contribution associated with the dominant translational mode.

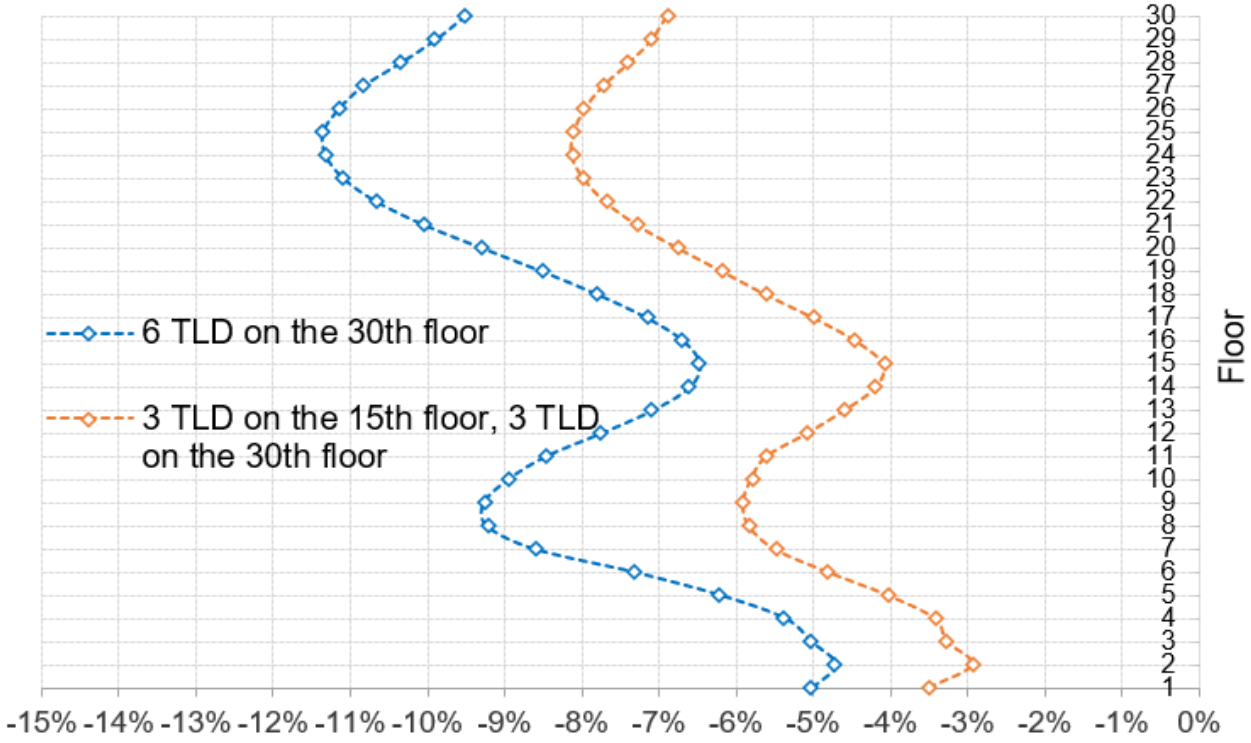


Fig. 11. Percentage reduction in floor absolute displacement (%)

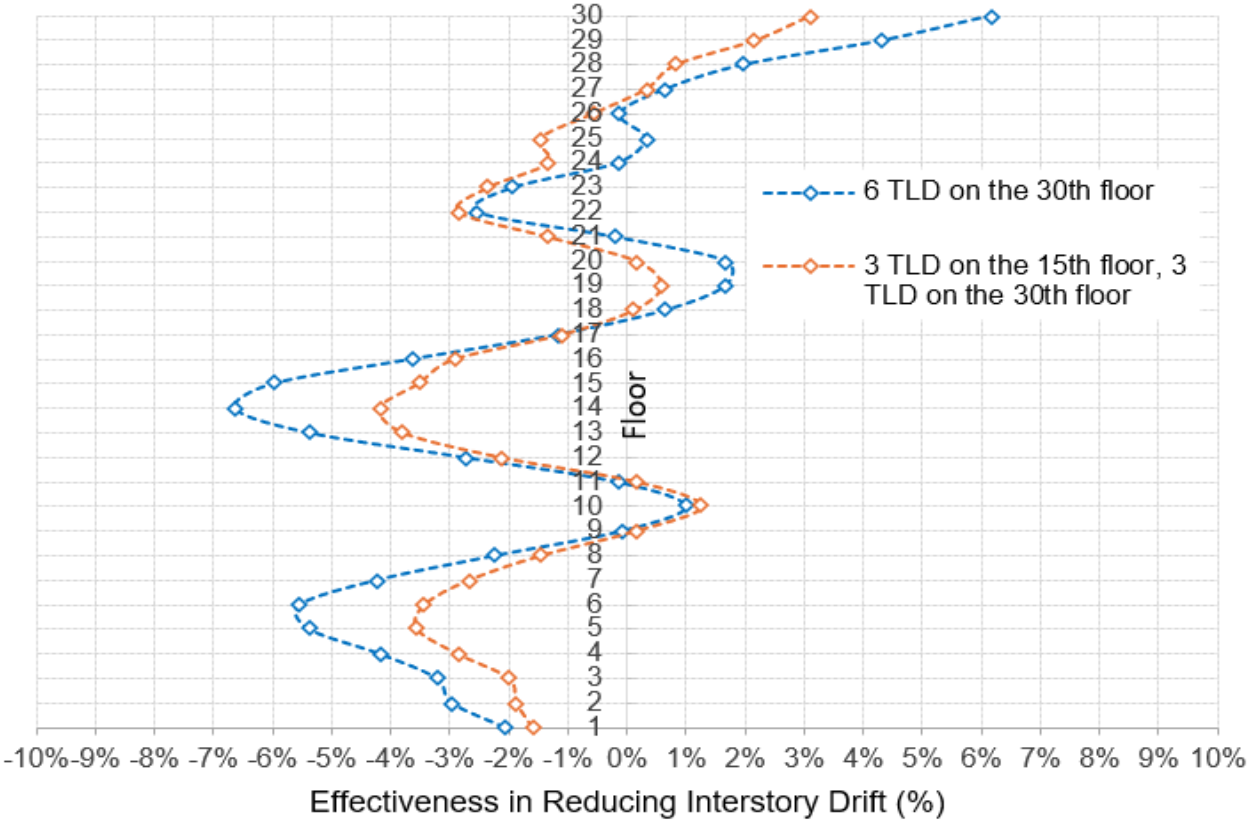


Fig. 12. Percentage change in interstory drift (%)

The fact that the largest percentage reduction occurs slightly below the roof rather than exactly at the top should not be interpreted as a loss of roof-level effectiveness. Instead, it reflects the combined effect of the modified modal shape and the normalization by the uncontrolled displacement at each floor. Although the absolute displacement is largest at the roof, the relative reduction ratio may reach a larger magnitude at adjacent upper stories where the difference between the controlled and uncontrolled modal profiles is proportionally greater.

The distributed configuration remains effective throughout the height but produces a lower global displacement reduction. Placing half of the liquid mass at the 15th floor decreases the generalized modal displacement imposed on those tanks because the first-mode amplitude at mid-height is lower than that at the roof. Therefore, the mid-height tanks contribute less to first-mode energy dissipation, even though they may interact more directly with local deformation in the middle stories.

5.3.2. Modification of interstory drift

The interstory-drift response in Fig. 12 exhibits a more irregular floorwise distribution than the absolute displacement response. This distinction is mechanically significant because absolute displacement is a global response quantity, whereas interstory drift is determined by the spatial gradient of the displacement profile. A relatively small modification of the modal shape may therefore produce a noticeable increase or decrease in drift at individual stories, even when the absolute displacement is reduced throughout the structure.

The greatest drift reductions occur in several localized regions, particularly around Floors 5–7 and 13–16. The roof-only configuration achieves reductions of approximately 6%–7% in these critical zones, while the distributed configuration generally produces smaller reductions of about 4%–5%. These reductions indicate that the TLDs flatten portions of the displacement profile and reduce the relative deformation between adjacent floors.

The concentration of drift improvement around the middle and lower-middle portions of the structure can be attributed to the curvature of the dominant modal shape. Interstory drift is related to the first spatial derivative of floor displacement; therefore, its reduction is governed not only by the decrease in global vibration amplitude but also by the manner in which the TLD modifies the slope of the displacement profile. The roof-mounted configuration suppresses the dominant mode more strongly and consequently reduces the displacement gradient over a wider range of stories.

Fig. 12 also shows small positive values at several upper and intermediate floors, indicating local drift amplification relative to the uncontrolled structure. This does not contradict the overall reduction in absolute displacement. The added water mass and the hydrodynamic coupling alter the effective mass, damping, and modal shape of the coupled system. As a result, deformation demand may be redistributed from one group of stories to another. A reduction in global displacement can therefore coexist with a slight local increase in the difference between two adjacent floor displacements.

These local amplifications are substantially smaller than the reductions observed in the principal drift-concentration regions. Nevertheless, they demonstrate that TLD performance should not be evaluated exclusively from roof displacement. Floorwise drift profiles are required to identify possible redistribution of deformation demand and to verify that vibration control does not shift excessive demand to isolated stories.

5.3.3. Modification of story shear

The story-shear response shown in Fig. 13 is more sensitive to TLD placement than the displacement response. Significant shear reductions are observed over several middle and

upper-middle stories, with the roof-only configuration reaching reductions of approximately 20%–25% around Floors 22–24. The distributed arrangement follows a similar trend but generally produces a smaller reduction.

The reduction in story shear results from the decrease in effective inertia forces after activation of the TLDs. During structural vibration, the sloshing liquid develops a hydrodynamic force that acts partly out of phase with the building motion. This counteracting force reduces the modal acceleration and consequently decreases the inertia forces transmitted through the lateral load-resisting system. Because story shear is the cumulative sum of floor inertia forces above a given level, changes in acceleration distribution can produce substantial variations in the shear envelope even when displacement reductions are comparatively moderate.

The pronounced reduction around Floors 21–24 suggests that the TLDs modify not only the amplitude but also the vertical distribution of modal inertia forces. In this region, the controlled and uncontrolled modal acceleration profiles diverge sufficiently to produce a marked decrease in cumulative shear. The stronger reduction produced by the roof-only configuration is consistent with its larger participation in the first mode and its greater ability to suppress the global acceleration response.

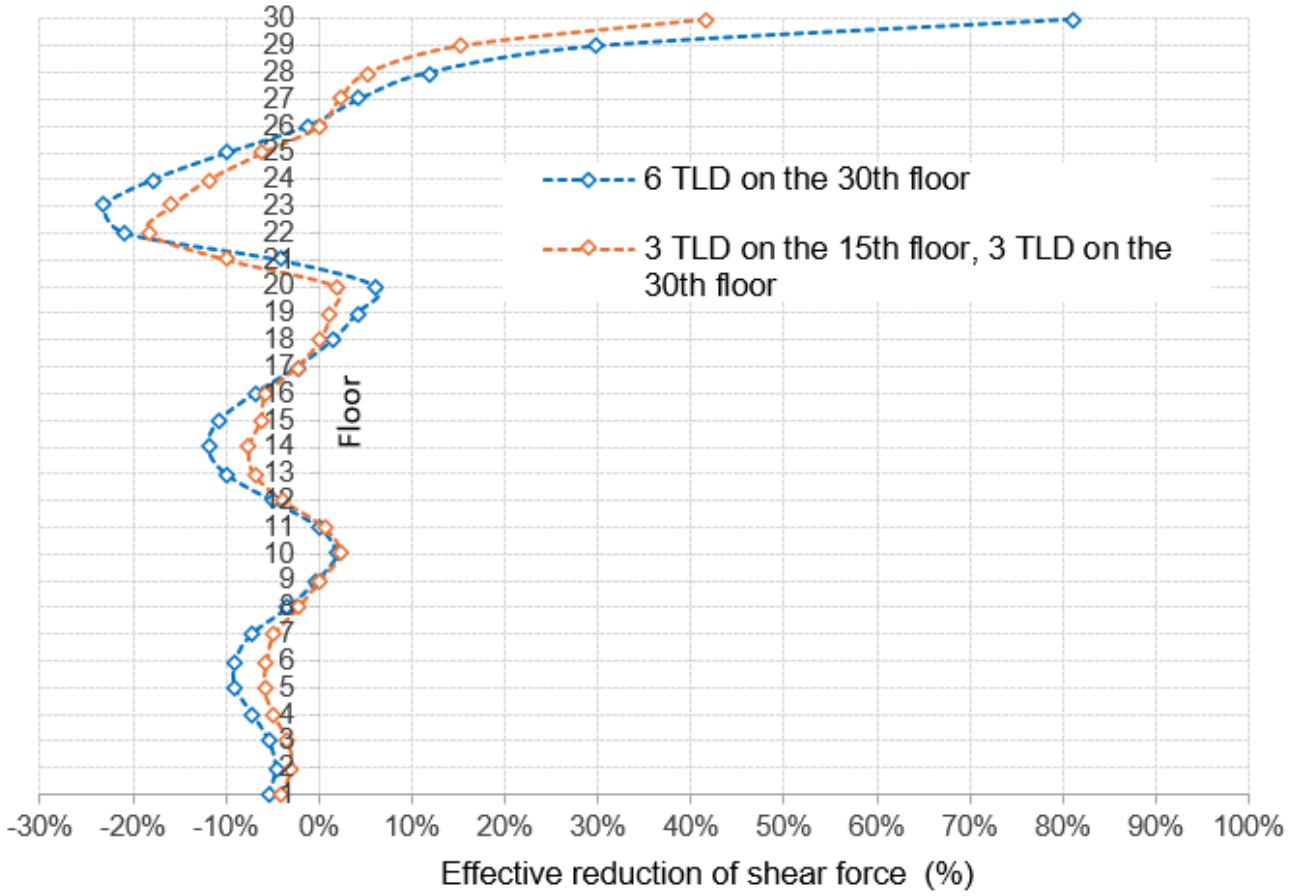


Fig. 13. Percentage change in story shear (%)

In contrast, Fig. 13 indicates positive response-change ratios at the uppermost floors, particularly for the six-roof-TLD configuration. These values represent local increases in the calculated shear envelope rather than reductions. Two factors contribute to this behavior. First, installing the tanks at the roof increases the concentrated mass at the top of the building. Second, the uncontrolled story shear near the roof is relatively small because only a limited amount of mass is located above these levels. Consequently, even a moderate change in local inertial force may

produce a large percentage variation when normalized by a small baseline value.

The large percentage increase near the roof should therefore be interpreted together with the corresponding absolute shear values. A high relative ratio at an upper floor does not necessarily imply that the shear demand there becomes critical compared with the much larger forces carried by the lower stories. However, it confirms that concentrating all TLD mass at the roof introduces a trade-off: it maximizes first-mode displacement control but may locally increase inertia-related force demand in the vicinity of the tank-supporting floors.

At the lower stories, the percentage reduction in shear is comparatively modest. This occurs because base and lower-story shears contain the accumulated contribution of nearly the entire structural mass. The hydrodynamic control force generated by the TLDs represents only part of this total inertia demand, and its relative influence becomes smaller as the cumulative mass contributing to story shear increases toward the base.

The results in Fig11–Fig13 demonstrate that TLD effectiveness is response-dependent and cannot be characterized by a single global reduction index. Absolute displacement is consistently reduced because it is predominantly governed by the fundamental translational mode. Interstory drift exhibits alternating reductions and minor local increases because it depends on changes in the slope of the displacement profile. Story shear is even more sensitive to the redistribution of modal acceleration and to the additional concentrated mass introduced by the tanks.

Among the two layouts, placing all six TLDs at the roof provides the strongest reduction in global displacement and generally produces greater reductions in critical drift and shear regions. This superior performance results from the maximum modal displacement and participation at the roof, which enhance structural–liquid energy exchange. The distributed configuration provides a more moderate response modification because the tanks at the 15th floor experience smaller first-mode motion. Nevertheless, distributing the liquid mass reduces the concentration of added mass at the roof and limits the local shear amplification observed near the upper stories.

Accordingly, the comparison reveals a mechanical trade-off between maximizing first-mode vibration suppression and controlling local force redistribution. The roof-only configuration is more effective for reducing the dominant global response, whereas the distributed arrangement provides a less concentrated modification of mass and inertia forces along the building height. These findings indicate that TLD placement should be selected by considering displacement, drift, and story-shear demands simultaneously rather than relying solely on roof-displacement reduction.

5.4. Assessment of Model Fidelity and Implications for Engineering Design

The numerical results should be interpreted in relation to the mechanical assumptions adopted in both the structural and fluid models. The reduced-order mass–spring–damper representation reproduces the dominant translational dynamics of the 30-story building with high accuracy and is therefore appropriate for evaluating first-mode-controlled responses such as roof displacement and the overall lateral deformation profile. However, the condensation of the detailed three-dimensional model into a planar reduced-order system inevitably suppresses several mechanisms that may become relevant under strong ground motion, including torsion–flexure coupling, diaphragm flexibility, local stiffness irregularities, and progressive material degradation. Consequently, the model is expected to provide reliable estimates of global response quantities, whereas local demands governed by higher modes, torsional response, or nonlinear stiffness deterioration should be interpreted with

greater caution.

A similar consideration applies to the hydrodynamic representation of the tuned liquid dampers. The FLUID80-based model captures the principal sloshing mode and the associated hydrodynamic pressure transfer, which are the dominant mechanisms governing TLD performance under moderate free-surface motion. Nevertheless, strongly nonlinear phenomena such as wave breaking, impact against tank walls, air entrainment, three-dimensional circulation, and turbulence-induced dissipation are not explicitly represented. These omitted mechanisms may alter both the phase and magnitude of the hydrodynamic force. In particular, additional viscous and turbulent dissipation could increase the effective damping of the real tank, whereas wave impact and strongly nonlinear free-surface motion could introduce localized force peaks that are not reproduced by the present formulation. The numerical predictions should therefore be regarded as representative of the principal structural–sloshing interaction rather than a complete description of all local fluid phenomena.

The comparison between the two TLD layouts further demonstrates that control effectiveness is governed by modal compatibility rather than by tank mass alone. The roof-only arrangement performs better in reducing global displacement because the roof corresponds to the location of maximum first-mode amplitude. At this elevation, the tank undergoes the largest support motion, producing stronger relative liquid movement and a larger out-of-phase hydrodynamic force. This enhances the transfer of seismic energy from the structure to the fluid and increases the generalized damping associated with the dominant translational mode.

By contrast, the distributed arrangement reduces the concentration of added mass at the roof and modifies the response over a broader range of elevations. The tanks installed at the 15th floor are subjected to a smaller first-mode displacement than those at the roof and therefore contribute less to global first-mode suppression. However, their intermediate location enables them to interact more directly with the local displacement gradients and modal curvature in the middle portion of the building. This explains why the distributed layout may provide localized benefits in interstory drift and shear, even though its reduction of roof displacement is less pronounced. The results therefore reveal a mechanical trade-off between maximizing first-mode coupling and achieving a more distributed modification of inertia forces and deformation demand.

This interpretation is also consistent with the floorwise response trends obtained in sections 5.2 and 5.3. Absolute displacement is reduced relatively smoothly because it is primarily controlled by the fundamental mode. Interstory drift exhibits more localized variations because it depends on the difference between adjacent floor displacements and is therefore sensitive to changes in modal slope and curvature. Story shear shows an even stronger dependence on the vertical distribution of modal acceleration, since it represents the cumulative inertia forces of the stories above a given level. Accordingly, the effectiveness of a TLD configuration cannot be evaluated solely from roof displacement; displacement, drift, acceleration, and story shear should be examined simultaneously to identify both global benefits and possible local response redistribution.

The response reductions obtained in the present study are broadly consistent with the ranges reported in classical TLD investigations. Fujino et al. (1992) reported vibration reductions of approximately 10%–25% for adequately tuned liquid dampers, while Reed et al. (1998) and Tait (2008) similarly demonstrated substantial response mitigation through experimental and numerical studies. This agreement supports the physical plausibility of the coupled ETABS–ANSYS framework. Nevertheless, consistency with

previous studies should not be interpreted as complete validation of all local response components, particularly those affected by higher-mode behavior, fluid nonlinearity, or structural yielding.

From an engineering design perspective, the results indicate that rooftop TLDs are particularly suitable for regular high-rise reinforced-concrete buildings whose seismic response is dominated by the fundamental translational mode. Existing rooftop water tanks may therefore be incorporated into a passive control strategy, provided that the sloshing frequency, liquid depth, tank geometry, mass ratio, and available freeboard are appropriately designed. For buildings with significant torsional sensitivity, vertical irregularity, or higher-mode contribution, a multi-level TLD arrangement may offer a more balanced distribution of control forces, although its total effectiveness will depend on the modal displacement at each installation level.

The present analysis was conducted for a fixed total liquid mass and a limited number of tank configurations. Therefore, the results identify the mechanical influence of placement but do not establish a universally optimal design. Further parametric investigation is required to determine the combined effects of mass ratio, tuning ratio, tank geometry, liquid depth, damping characteristics, and vertical distribution. Experimental or high-fidelity nonlinear FSI validation would also be valuable for assessing wave impact, turbulence, and possible detuning under large-amplitude seismic excitation.

The adopted modeling strategy captures the principal mechanisms governing global structural–TLD interaction and provides a computationally efficient basis for comparing alternative tank layouts. The findings demonstrate that concentrating the TLD mass at the roof maximizes first-mode vibration suppression, whereas distributing the tanks modifies local deformation and inertia-force patterns over a wider height range. This distinction is important for design because the most effective configuration depends not only on the desired reduction in roof displacement but also on the acceptable redistribution of interstory drift and story shear.

6. Conclusion

This study developed a hybrid numerical framework for the seismic analysis of high-rise reinforced concrete buildings equipped with tuned liquid dampers (TLDs). The proposed approach integrates a detailed three-dimensional structural model, a reduced-order structural model, and a three-dimensional fluid–structure interaction (FSI) model, providing an efficient tool for evaluating structural–TLD interaction under earthquake excitation.

The validation results demonstrate that the reduced-order model accurately reproduces the dominant dynamic characteristics of the detailed structural model, with a fundamental frequency error below 0.2%. This confirms that the simplified model provides sufficient accuracy for predicting global seismic responses while significantly reducing computational cost.

The seismic analyses reveal that TLD effectiveness is primarily governed by the compatibility between tank location and the dominant structural mode. Concentrating all tanks at the roof achieves the greatest reduction in global displacement by maximizing first-mode energy dissipation, whereas the distributed configuration provides a more balanced modification of interstory drift and story shear over the building height. These findings indicate that the effectiveness of TLD systems depends not only on the liquid mass but also on its vertical distribution within the structure.

Overall, the proposed framework provides a mechanically consistent and computationally efficient approach for evaluating TLD configurations in high-rise buildings. Future work should consider structural material nonlinearity, strongly nonlinear sloshing behavior, and broader parametric investigations to optimize TLD design

under different seismic conditions.

Declaration of Generative AI

The authors used ChatGPT (OpenAI) solely to refine the language and improve the readability of the manuscript. The authors developed and verified all scientific analyses, interpretations, and conclusions and take full responsibility for the final content.

References

[1] B.R. Ellis. (1980). An assessment of the accuracy of predicting the fundamental natural frequencies of buildings and the implications concerning the dynamic analysis of structures. *Proceedings of the Institution of Civil Engineers*, 69(3), 763–776. https://doi.org/10.1680/iicep.1980.2376

[2] T.K. Datta. (2010). Seismic Analysis of Structures. *John Wiley & Sons*. https://doi.org/10.1002/9780470824634

[3] G.W. Housner, L.A. Bergman, T.K. Caughey, A.G. Chassiakos, R.O. Claus, S.F. Masri, R.E. Skelton, T.T. Soong, B.F. Spencer, J.T.P. Yao. (1997). Structural control: Past, present, and future. *Journal of Engineering Mechanics*, 123(9), 897–971. https://doi.org/10.1061/(ASCE)0733-9399(1997)123:9(897)

[4] Y. Fujino, L. Sun, B.M. Pacheco, P. Chaiseri. (1992). Tuned liquid damper (TLD) for suppressing horizontal motion of structures. *Journal of Engineering Mechanics*, 118(10), 2017–2030. https://doi.org/10.1061/(ASCE)0733-9399(1992)118:10(2017)

[5] M.J. Tait. (2008). Modelling and preliminary design of a structure–TLD system. *Engineering Structures*, 30(10), 2644–2655. https://doi.org/10.1016/j.engstruct.2008.02.017

[6] D. Reed, J. Yu, H. Yeh, S. Gardarsson. (1998). Investigation of tuned liquid dampers under large amplitude excitation. *Journal of Engineering Mechanics*, 124(4), 405–413. https://doi.org/10.1061/(ASCE)0733-9399(1998)124:4(405)

[7] Y. Fujino, L.M. Sun. (1993). Vibration control by multiple tuned liquid dampers (MTLDs). *Journal of Structural Engineering*, 119(12), 3482–3502. https://doi.org/10.1061/(ASCE)0733-9445(1993)119:12(3482)

[8] K.W. Min, H.S. Kim, S.H. Lee, H. Kim, S.K. Ahn. (2005). Performance evaluation of tuned liquid column dampers for response control of a 76-story benchmark building. *Engineering Structures*, 27(7), 1101–1112. https://doi.org/10.1016/j.engstruct.2005.02.008

[9] M. Mohebbi, H.R. Dabbagh, K. Shakeri. (2015). Optimal design of multiple tuned liquid column dampers for seismic vibration control of MDOF structures. *Periodica Polytechnica Civil Engineering*, 59(4), 543–558. https://doi.org/10.3311/PPci.7645

[10] H. Gao, K.C.S. Kwok, B. Samali. (1997). Optimization of tuned liquid column dampers. *Engineering Structures*, 19(6), 476–486. https://doi.org/10.1016/S0141-0296(96)00099-5

[11] A. Das, T. Konar, D. Maity, S.K. Bhattacharyya. (2023). Revisiting equivalent tuned mass damper analogy for tuned liquid damper utilizing CFD–FEA framework. *Soil Dynamics and Earthquake Engineering*, 172, 108051. https://doi.org/10.1016/j.soildyn.2023.108051

[12] X. Wen, X. Chen, D. Wan. (2017). MPS simulation of sloshing flows in a tuned liquid damper. *Proceedings of the 27th International Ocean and Polar Engineering Conference, USA, pp. 1009–1016. International Society of Offshore and Polar Engineers (ISOPE).*

[13] C.R. Chu, Y.R. Wu, T.R. Wu, C.Y. Wang. (2018). Slosh-induced hydrodynamic force in a water tank with multiple baffles. *Ocean Engineering*, 167, 282–292. https://doi.org/10.1016/j.oceaneng.2018.08.049

[14] B.P.D. Tuong, P.D. Huynh, T.-T. Bui, V. Sarhosis. (2019). Numerical analysis of the

dynamic responses of multistory structures equipped with tuned liquid dampers considering fluid–structure interactions. *The Open Construction and Building Technology Journal*, 13, 289–300. https://doi.org/10.2174/1874836801913010289

[15] M. Eswaran, S. Athul, P. Niraj, G.R. Reddy, M.R. Ramesh. (2017). Tuned liquid dampers for multi-storey structure: Numerical simulation using a partitioned FSI algorithm and experimental validation. *Sādhanā,* 42(4), 449–465. https://doi.org/10.1007/s12046-017-0614-z

[16] M.U. Shah, M. Usman. (2022). An experimental study of tuned liquid column damper controlled multi-degree of freedom structure subject to harmonic and seismic excitations. *PLOS ONE*, 17(6), e0269910. https://doi.org/10.1371/journal.pone.0269910

[17] T.T. Hoa, N.T.T. Trinh. (2022). Studying the influence of bearing stiffness between liquid storage tanks and high-rise building structures subject to earthquake effects. *Journal of Transport*, 1+2, 58-63. (in Vietnamese).

[18] T.H. Trinh, T.T.T. Nguyen. (2022). Optimized design of tuned liquid damper for mitigating seismic induced vibration in case of high-rise building. *CIGOS 2021—Emerging Technologies and Applications for Green Infrastructure. Lecture Notes in Civil Engineering, vol. 203, pp. 431–439. Springer*. https://doi.org/10.1007/978-981-16-7160-9_43

[19] T.T. Hoa, T.T.T. Nguyen. (2020). An overview of calculating methods for fluid damping (TLD). *Journal of Transport*, 3, 40-44. (in Vietnamese).

[20] T.T. Hoa, N.T.T. Trinh, N.T. Chuong, T.A. Nguyen. (2020). Application of Ansys software to analyze the interaction in the water tank under the effect of the harmonic load with the impact of water waves in the tank taken into account. *Journal of Transport*, 8, 28-32. (in Vietnamese).

[21] G.W. Housner. (1963). The dynamic behavior of water tanks. *Bulletin of the Seismological Society of America*, 53(2), 381–387. https://doi.org/10.1785/BSSA0530020381

[22] S. Adhikari, A. Phani. (2007). Rayleigh's classical damping revisited. *Proceedings of the International Conference on Civil Engineering in the New Millennium: Opportunities and Challenges.*

[23] A.R. Ghaemmaghami, M.R. Kianoush. (2010). Effect of wall flexibility on dynamic response of concrete rectangular liquid storage tanks under horizontal and vertical ground motions. *Journal of Structural Engineering*, 136(4), 441–451. https://doi.org/10.1061/(ASCE)ST.1943-541X.0000123

[24] A.R. Ghaemmaghami, M. Moslemi, R. Kianoush. (2010). Dynamic behaviour of concrete liquid tanks under horizontal and vertical ground motions using finite element method. *Proceedings of the 9th U.S. National and 10th Canadian Conference on Earthquake Engineering, Paper No. 1324.*

[25] ANSYS, Inc. (2017). ANSYS Academic Research Mechanical, Release 18.1, Help System, Coupled Field Analysis Guide. *ANSYS, Inc., USA*.

[26] Ministry of Science and Technology (Vietnam). (2012). TCVN 9386:2012—Design of Structures for Earthquake Resistances. Part 1: General Rules, Seismic Actions and Rules for Buildings; Part 2: Foundations, Retaining Structures and Geotechnical Aspects. (in Vietnamese).

[27] Ministry of Science and Technology (Vietnam). (2023). TCVN 2737:2023—Loads and Actions. (in Vietnamese).

[28] A.D. Nguyen. (2019). Method for determining the natural vibration period of multistory buildings. *HUAF Journal of Agricultural Science & Technology*, 3(2), 1337–1348. https://doi.org/10.46826/huaf-jasat.v3n2y2019.256. (in Vietnamese).

[29] T.C. Nguyen. (2015). Structural Analysis of Multistory Buildings. *Construction Publishing House, Vietnam. ISBN 978-604-82-2656-5.* (in Vietnamese).

[30] B.T. Vo. (2012). High-Rise Buildings in Reinforced Concrete. *Vietnam National University Ho Chi Minh City Press, Ho Chi Minh City, Vietnam.* (in Vietnamese).

[31] Vibrationdata. (n.d.). El Centro Earthquake (1940): North–South Component, Acceleration Time-History Data. Available at: https://www.vibrationdata.com/elcentro.htm (accessed 8 July 2026).